

Syntheses, characterization, and energy transfer properties of benzothiadiazole-based hyperbranched polyfluorenes

Zhun Ma^a, Su Lu^b, Qu-Li Fan^{c,*}, Chun-Yang Qing^a, Yan-Yan Wang^a,
Pei Wang^a, Wei Huang^{a,c,**}

^a Institute of Advanced Materials (IAM), Fudan University, 220 Handan Road, Shanghai 200433, China

^b Institute of Materials Research and Engineering (IMRE), National University of Singapore, 3 Research Link, Singapore 117602, Singapore

^c Institute of Advanced Materials (IAM), Nanjing University of Posts and Telecommunications, 66 New Mofan Road, Nanjing 210003, Jiangsu, China

Received 25 March 2006; received in revised form 11 July 2006; accepted 5 August 2006

Available online 8 September 2006

Abstract

A series of benzothiadiazole-based (BT) hyperbranched polyfluorene copolymers with various branching degrees (5–40%) were designed and synthesized. TGA and film annealing tests showed the substantial thermal stability of these highly branched polymers. The optical performance of the polymers in solutions and as films, and their electrochemical properties were characterized. The energy transfer (ET) processes in these hyperbranched conjugated polymers, both in solutions and in the solid state, were also investigated. With the change of the solution concentration and the branching degree, the energy transfer efficiency of the polymers varied in solutions and the main photoluminescence (PL) peaks changed from blue to green region. As films, only green light emitted from BT units. In addition, the PL efficiency of the films decreased dramatically with the increase of branching degrees. All these features demonstrated that highly branched structure would effectively impede the intra- and interchain energy migration, especially in solutions, and remarkably influence the ET process in the solid state, which resulted in low PL efficiency.

© 2006 Elsevier Ltd. All rights reserved.

Keywords: Conjugated polymer; Hyperbranched structure; Energy transfer

1. Introduction

Polymer light-emitting diodes have the potential to become the main display products in the future since they have many advantages regarding preparation and operation over other display systems [1–3]. Three primary colors, i.e. blue, green, and red-emitting materials, are essential for full-color displays. Among those polymer light-emitting materials, polyfluorene (PF) and its derivatives have emerged as the most promising ones due to their emission at wavelength spanning the entire visible

spectrum, high fluorescence efficiency, and good thermal stability [4–6]. Because of its higher band gap property, fluorene is often used as energy donor for copolymerization or blending to realize green or red light emitting [7,8]. One successful method for obtaining color tuning was the doping of green- or red-emitting materials into PFs. But there are some disadvantages for this method such as phase separation.

In the past few years, copolymerization of fluorene with lower band gap comonomers has become more and more popular. Among many other progresses, Inbasekaran et al. have reported several fluorene-based copolymers synthesized by alternating copolymerization using 5,5'-dibromo-2,2'-bithiophene and 4,7-dibromo-2,1,3-benzothiadiazole, which showed yellow and green emissions, respectively [9]. Cao et al. have also reported a series of red light-emitting copolymers derived from fluorene and 4,7-di-2-thienyl-2,1,3-benzothiadiazole or 2-pyran-4-ylidenemalononitrile [10,11].

* Corresponding author.

** Corresponding author. Institute of Advanced Materials (IAM), Fudan University, 220 Handan Road, Shanghai 200433, China. Tel.: +86 21 5566 4188/4198; fax: +86 21 6565 5123/5566 4192.

E-mail addresses: qlfan@fudan.edu.cn (Q.-L. Fan), wei-huang@njupt.edu.cn, chehw@nus.edu.sg (W. Huang).

It was observed that a small amount (usually <5 mol%) of comonomers in the copolymers was sufficient to change the blue emission of PF to yellow, green or red emission. In these copolymers or blends, polyfluorene family acted as energy donors. Thus, investigations on energy transfer (ET) processes from donors to acceptors in conjugated oligomers and polymers are very important and there are numerous reports on energy transfer through linear conjugated structures [12–16].

In the meantime, because of their unusual molecular structures and properties, dendrimers and hyperbranched polymers have received considerable attention as light-emitting materials [17–20]. Highly branched and globular features depress the aggregation and excimer formation so as to improve the light-emitting efficiencies and also make the materials to form good quality amorphous films. Moreover, novel hyperbranched structure brings specific photophysical properties in solution and in the solid state [21,22]. But energy transfer mechanism in this highly branched structure is far from clear definition.

In this study, we introduced different contents of branching units into the poly(fluorene-*co*-benzothiazole) to construct the copolymers of a hyperbranched structure. Furthermore, the energy transfer properties and their correlation with PL efficiencies of hyperbranched conjugated copolymers were studied. The narrow band gap comonomer 2,1,3-benzothiadiazole (BT) acts as a powerful exciton trap which allows efficient energy transfer of the exciton from fluorene segment to BT unit in the copolymers. As a result, the blue emission from the fluorene segment is completely quenched in concentrated solutions and in the solid state. But with the change of the solution concentration and the branching degree (BD) which is defined as the initial feed ratio of branching units [17], the efficiency of energy transfer of these hyperbranched polymers varied in solutions. These results demonstrated that highly branched structure would effectively impede the intra- and interchain energy migration, especially in solutions, and remarkably influence the ET process in the solid state. The dynamics of energy transfer in solutions and as solid-state films of these hyperbranched polymers are still under investigation in our group and will be reported elsewhere.

2. Experimental section

2.1. Measurements

^1H and ^{13}C NMR spectra were recorded on a Varian Mercury Plus 400 in CDCl_3 solution with tetramethylsilane as reference. The gel permeation chromatography (GPC) measurements were performed on a Shimadzu LC10A chromatograph with THF as an eluent and polystyrenes as external standards. UV–vis absorption spectra were obtained on a Shimadzu UV–vis spectrometer model UV-3150. Photoluminescence (PL) data were recorded on a Shimadzu RF-5300PC. Elemental analyses were performed on a Vario EL elemental analysis instrument (Elementar Co.). TGA (Shimadzu DTG-60H) measurements were carried out under a nitrogen atmosphere at a heating rate of $10\text{ }^\circ\text{C}/\text{min}$. Cyclic voltammetry was carried out on a CHI660A

electrochemical workstation in a solution of tetrabutylammonium hexafluorophosphate (Bu_4NPF_6) (0.1 M) in acetonitrile at a scan rate of 50 mV/s at room temperature under the protection of argon. Measurement of the absolute PL efficiency was performed on LabsphereIS-080 ($8''$), which contained an integrating sphere coated on the inside with a reflecting material barium sulfate, and the diameter of the integrating sphere was 8 inch. PL efficiency was calculated from the software attached by LabsphereIS-080 ($8''$).

2.2. Materials

All manipulations involving air-sensitive reagents were performed under an atmosphere of dry argon. All reagents, unless otherwise specified, were obtained from Aldrich and Acros Chemical Co. and used as received. All the solvents used were further purified before use. Acetonitrile used in the electrochemical measurements was refluxed in the presence of calcium hydride under argon and distilled prior to use.

2.3. Synthesis of monomers

2.3.1. 2-(3,5-Dibromo-phenyl)-[1,3,2]dioxaborin (2)

Compound **2** was prepared from **1** following the procedures reported in the literature [23]. The boronic ester was purified by recrystallization using hexane and acetone (4:1) as solvent and dried under vacuum. The overall yield of the colorless solid was 73% (starting from 1,3,5-tribromobenzene). ^1H NMR (400 MHz, CDCl_3) δ (ppm): 7.79 (s, 2H), 7.69 (s, 1H), 4.15 (t, 4H), 2.05 (m, 2H). ^{13}C NMR (100 MHz, CDCl_3) δ (ppm): 135.98, 135.32, 122.94, 62.36, 27.50.

2.3.2. 2-([1,3,2]Dioxaborolan-2'-yl)-7-bromo-9,9-bis(*n*-octyl)fluorene (4)

Compound **4** was made from **3** according to the procedure for the synthesis of **2** as a white powder. Yield: 70% (starting from 2,7-dibromo-9,9-bis(*n*-octyl)fluorene). ^1H NMR (400 MHz, CDCl_3) δ (ppm): 7.76 (d, 1H), 7.70 (s, 1H), 7.64 (d, 1H), 7.55 (d, 1H), 7.42 (d, 2H), 4.20 (t, 4H), 2.09 (m, 2H), 1.95 (d, 4H), 1.26–1.03 (m, 20H), 0.83 (t, 6H), 0.56 (m, 4H). ^{13}C NMR (100 MHz, CDCl_3) δ (ppm): 153.76, 149.55, 142.59, 140.38, 132.82, 130.03, 128.06, 126.37, 121.55, 121.47, 119.15, 62.26, 55.55, 40.48, 32.03, 30.20, 29.95, 29.46, 29.43, 27.67, 23.87, 22.84, 14.33.

2.3.3. 4,7-Dibromo-2,1,3-benzothiadiazole (5)

2,1,3-Benzothiadiazole (5.0 g, 36.7 mmol) in 13 mL of 40% HBr solution was heated to reflux while bromine (17.6 g, 5.6 mL, 110.0 mmol) was added dropwise. At the end of the addition, an extra 8.6 mL of HBr was added, and the mixture was heated under reflux for an additional 3 h. The mixture was filtered while hot, and the filtrate was washed with water, 5% sodium bicarbonate and water. The crude product was collected, dried, and recrystallized from chloroform–hexane to afford 4,7-dibromo-2,1,3-benzothiadiazole (7.2 g, 67%) as gray crystals. ^1H NMR (400 MHz, CDCl_3) δ (ppm): 7.73. ^{13}C NMR (100 MHz, CDCl_3) δ (ppm): 153.18, 132.57, 114.13.

2.3.4. 9,9-Bis(*n*-octyl)fluoren-2-yl-boronic acid (**6**)

Into a solution of 2-bromo-9,9-bis(*n*-octyl)fluorene (15.3 g, 32.6 mmol) in anhydrous THF (120 mL) was added *n*-BuLi (26.5 mL, 42.4 mmol) at -78°C . The reaction mixture was stirred for 1 h before tri-*iso*-propyl borate (17.8 mL, 65.2 mmol) was added in one portion. The mixture was warmed to room temperature, stirred overnight and then quenched with HCl (2.0 M, 125 mL) before adding a large amount of water for extraction with ethyl ether. The organic extracts were washed with brine and dried over Na_2SO_4 . Upon evaporating off the solvent, the residue was purified with column chromatography on silica gel with petroleum ether:ethyl acetate (3:1) as the eluent to afford **6** as white solids (12.7 g, 90%). ^1H NMR (400 MHz, CDCl_3) δ (ppm): 8.33 (d, 1H), 8.23 (s, 1H), 7.90 (d, 1H), 7.72 (m, 1H), 7.36–7.43 (m, 3H), 2.16–1.93 (m, 4H), 1.28–1.00 (m, 20H), 0.83 (m, 6H), 0.72 (broad, 2H), 0.60 (broad, 2H). ^{13}C NMR (100 MHz, CDCl_3) δ (ppm): 151.91, 150.39, 145.89, 141.02, 134.94, 129.98, 128.20, 127.11, 123.29, 120.67, 119.55, 55.35, 40.70, 32.12, 30.39, 29.58, 29.55, 24.12, 22.91, 14.35.

2.4. Polymerization

2.4.1. General procedure of polymerization

Carefully purified 2-([1,3,2]dioxaborolan-2'-yl)-7-bromo-9,9-bis(*n*-octyl)fluorene (**4**), 2-(3,5-dibromo-phenyl)-[1,3,2]dioxaborin (**2**), 4,7-dibromo-2,1,3-benzothiadiazole (**5**), $\text{Pd}(\text{PPh}_3)_4$ (1.5–2.0 mol%), and several drops of Aliquat 336 were dissolved in a mixture of toluene and aqueous 2 M Na_2CO_3 . The mixture was refluxed with stirring for 3 days under argon atmosphere, then 9,9-bis(*n*-octyl)fluoren-2-yl-boronic acid (**6**) and additional $\text{Pd}(\text{PPh}_3)_4$ were added and the mixture was further stirred and refluxed for 2 days. The reaction mixture was then cooled to room temperature and some amount of thiourea was added and then the mixture was vigorously stirred for another 3 h. The mixture was filtrated to remove the catalyst residues and after removal of the solvent, the residue was then dissolved in a minimum of CHCl_3 and the solution was dropped into methanol. The formed precipitate was recovered by filtration. The solid was washed with methanol, water, and then again with methanol. The resulting polymers were collected and dried under vacuum.

2.4.2. Linear poly(fluorene-co-benzothiadiazole) LPFBT

Compound **4** (0.5 g, 0.90 mmol), **5** (13.9 mg, 0.047 mmol), 2 M Na_2CO_3 aq. (4.5 mL, 9 mmol), and toluene (15 mL) were carefully degassed before and after $\text{Pd}(\text{PPh}_3)_4$ (15.6 mg, 0.0135 mmol) was added. The mixture was stirred and refluxed for 3 days, then **6** (0.56 g, 1.29 mmol) and additional $\text{Pd}(\text{PPh}_3)_4$ were added and the mixture was further stirred and refluxed for 2 days. Yield: 83%. ^1H NMR (400 MHz, CDCl_3) δ (ppm): 8.08, 8.01, 7.94, 7.86–7.84, 7.72–7.66, 7.62–7.60, 7.54–7.46, 2.25–1.93, 1.26–1.13, 0.87–0.80. Element Anal. Found: C, 88.05%; H, 10.07%; N, 0.86%; S, 0.99%.

2.4.3. Hyperbranched polymer HPFBT_B5

A mixture of **4** (0.6 g, 1.08 mmol) **2** (18.2 mg, 0.057 mmol), **5** (16.8 mg, 0.057 mmol), 2 M Na_2CO_3 aq. (5.4 mL,

10.8 mmol) and toluene (15 mL) was carefully degassed before and after $\text{Pd}(\text{PPh}_3)_4$ (16.4 mg, 0.0142 mmol) was added. The mixture was stirred and refluxed for 3 days, then **6** (0.657 g, 1.51 mmol) and additional $\text{Pd}(\text{PPh}_3)_4$ were added and the mixture was further stirred and refluxed for 2 days. Yield: 76%. ^1H NMR (400 MHz, CDCl_3) δ (ppm): 8.09, 8.02, 7.94, 7.86–7.84, 7.77–7.65, 7.62–7.59, 7.53–7.46, 2.24–1.96, 1.26–1.14, 0.83–0.72. Element Anal. Found: C, 88.57%; H, 9.62%; N, 0.82%; S, 0.98%.

2.4.4. Hyperbranched polymer HPFBT_B15

A mixture of **4** (0.6 g, 1.08 mmol), **2** (54.5 mg, 0.17 mmol), **5** (16.8 mg, 0.057 mmol), 2 M Na_2CO_3 aq. (5.4 mL, 10.8 mmol) and toluene (15 mL) was carefully degassed before and after $\text{Pd}(\text{PPh}_3)_4$ (18.7 mg, 0.0162 mmol) was added. The mixture was stirred and refluxed for 3 days, then **6** (0.657 g, 1.51 mmol) and additional $\text{Pd}(\text{PPh}_3)_4$ were added and the mixture was further stirred and refluxed for 2 days. Yield: 64%. ^1H NMR (400 MHz, CDCl_3) δ (ppm): 8.09, 8.01, 7.94, 7.86–7.84, 7.77–7.66, 7.62–7.60, 7.52–7.46, 2.22–1.98, 1.26–1.14, 0.82–0.72. Element Anal. Found: C, 88.02%; H, 10.05%; N, 0.86%; S, 0.96%.

2.4.5. Hyperbranched polymer HPFBT_B40

A mixture of **4** (0.6 g, 1.08 mmol), **2** (0.14 g, 0.45 mmol), **3** (16.8 mg, 0.057 mmol), 2 M Na_2CO_3 aq. (5.4 mL, 10.8 mmol) and toluene (15 mL) was carefully degassed before and after $\text{Pd}(\text{PPh}_3)_4$ (16.4 mg, 0.0142 mmol) was added. The mixture was stirred and refluxed for 3 days, then **6** and additional $\text{Pd}(\text{PPh}_3)_4$ were added and the mixture was further stirred and refluxed for 2 days. Yield: 56%. ^1H NMR (400 MHz, CDCl_3) δ (ppm): 8.09, 8.01, 7.94, 7.87–7.84, 7.78–7.65, 7.62–7.60, 7.54–7.47, 2.20–1.93, 1.26–1.10, 0.82–0.71. Element Anal. Found: C, 87.92%; H, 9.79%; N, 0.82%; S, 0.87%.

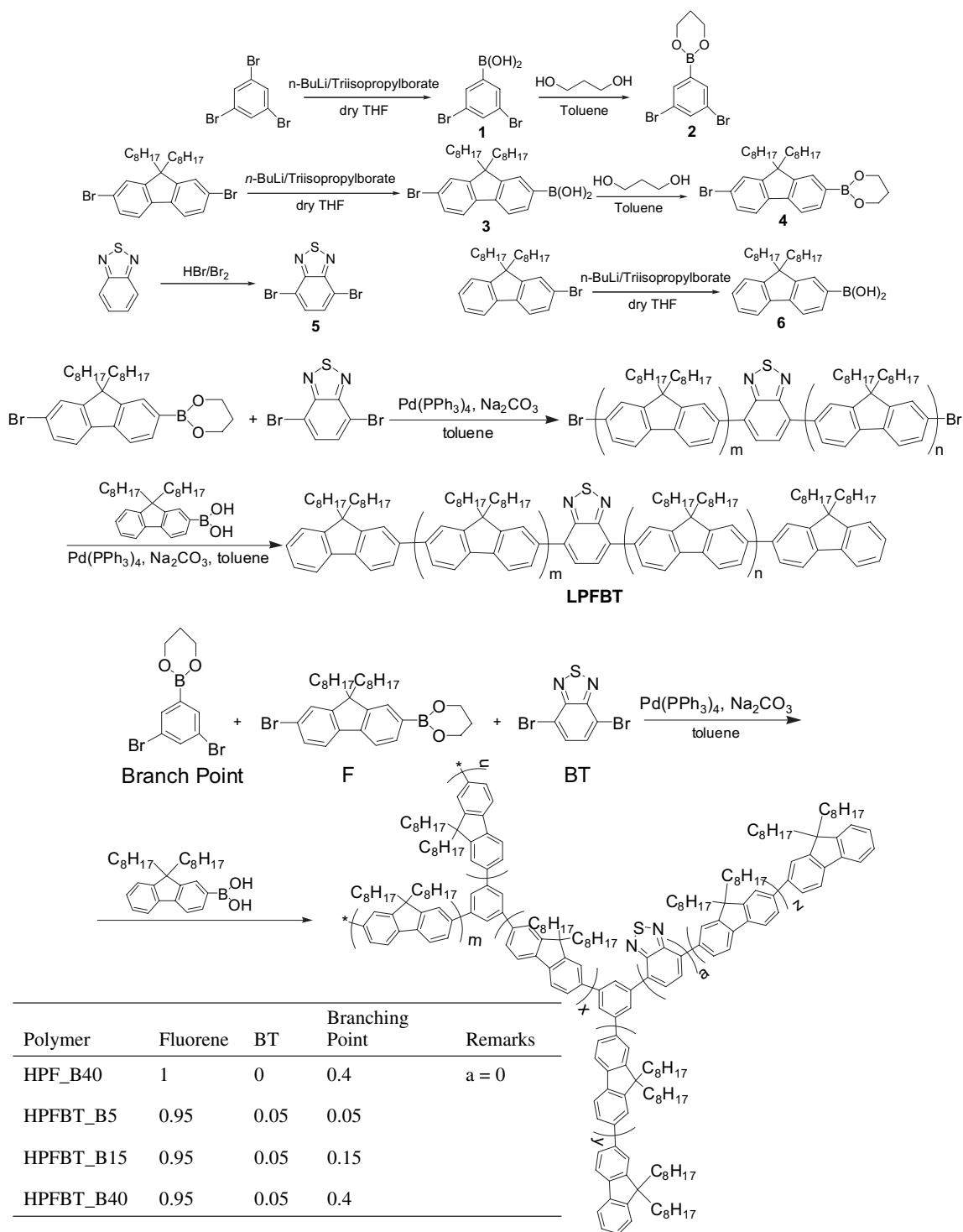
2.4.6. Hyperbranched polyfluorene HPF_B40

A mixture of **4** (0.6 g, 1.08 mmol), **2** (0.139 g, 0.434 mmol), 2 M Na_2CO_3 aq. (7.18 mL, 14.36 mmol), and toluene was carefully degassed before and after $\text{Pd}(\text{PPh}_3)_4$ (12.5 mg, 0.0108 mmol) was added. The mixture was stirred and refluxed for 3 days, then **6** and additional $\text{Pd}(\text{PPh}_3)_4$ were added and the mixture was further stirred and refluxed for 2 days. Yield: 62%. ^1H NMR (400 MHz, CDCl_3) δ (ppm): 7.87–7.80, 7.78–7.74, 7.70–7.63, 7.60–7.59, 7.49, 2.19–1.89, 1.26–1.09, 0.86–0.70. Element Anal. Found: C, 90.01%; H, 9.92%.

3. Results and discussion

3.1. Synthesis and characterization

The synthetic route is shown in Scheme 1. (3,5-Dibromophenyl)boronic acid (**1**) [24], 7-bromo-9,9-bis(*n*-octyl)fluoren-2-yl-boronic acid (**3**) [25], 4,7-dibromo-2,1,3-benzothiadiazole (**5**) [26], and 9,9-bis(*n*-octyl)fluoren-2-yl-boronic



Scheme 1. Synthetic route of the monomers and polymers.

acid (**6**) [27] were prepared according to the literature procedures.

Suzuki polycondensations (SPC) with **2**, **4**, and **5** were conducted in biphasic system (toluene/aqueous Na_2CO_3) with $\text{Pd}(\text{PPh}_3)_4$ as a catalyst precursor. The reactions were kept stirring at reflux temperature for 3 days. Then, end-capped group **6** was added to reduce the heavy atom effect which quenched fluorescence [28]. All of the linear or hyperbranched polymers

(LPFBT, HPF_B40, HPFBT_B5, B15 and B40) could be fully dissolved in common organic solvents, such as chloroform, toluene, methylene chloride, and THF. Standard workup afforded the polymers as amorphous, yellow solids, except HPF_B40 which is grayish. The crude polymers were redissolved in certain amount of CHCl_3 , which was added dropwise to methanol so as to precipitate the high molar mass polymers. The fractionated high molar mass polymers were separated by

Table 1
Molecular weights, thermal properties, and fluorescence quantum yield of the linear and hyperbranched polymers

Polymer	M_n (kDa)	M_w (kDa)	PI	Yield ^a (%)	T_d (°C)	$\eta_{PL}^{b,c}$ (%)
LPFBT	7.3	13.1	1.80	83	280	38.8
HPF_B40	7.8	13.7	1.76	62	366	45.4
HPFBT_B5	6.6	16.5	2.50	76	294	33.9
HPFBT_B15	8.5	17.5	2.06	64	335	29.5
HPFBT_B40	7.0	12.0	1.71	56	376	16.5

^a Isolated yield.

^b All polymers were excited at 378 nm.

^c PL efficiencies in the solid state.

filtration and dried in vacuum glass oven. The molecular weights determined by gel permeation chromatography (GPC) are summarized in Table 1. The molecular weights are not very high which may be due to unequal quantity of reactive groups for bromo and borate. In our polymerization reactions, the feed ratios of bromo to borate are from 1.10 to 1.37.

The BT content of the resulted polymers was measured by elemental analysis. The S or N contents of the polymers indicate that the BT contents in linear or hyperbranched copolymers are close to the monomers feed ratio of BT/fluorene. With ¹H NMR spectra, the peak areas around 2 ppm (–CH₂ bounded to 9 position of fluorene) were used to determine the ratios of fluorene in copolymers. Thus, the peak areas corresponding to branching units were calculated to deduct the relevant fluorene and BT peak areas from all peak intensities from 7.9 to 7.4. For polymers HPF_B40, HPFBT_B5, B15 and B40, the amounts of branching units are calculated as approximately 33, 2, 9, and 29%, respectively.

3.2. Thermal properties

All the polymers were characterized by thermal gravimetric analysis (TGA) and the results are listed in Table 1. The polymers with BDs above 15% exhibited good thermal stability and showed 5% decomposition at around 360 °C. As for linear and 5% branching degree polymers, a major degradation onset could be observed at around 290 °C. It can be concluded that higher branching degree leads to higher thermal stability, which is one of the advantages of hyperbranched polymers.

Table 2
Optical properties of linear and hyperbranched polymers

Polymer	Solution		Film			
	UV (nm)	PL (nm)	UV, λ_{max} (nm)		PL, λ_{max} (nm)	
	λ_{max}	λ_{max}^a	As-sp ^b	Ann ^c	As-sp ^b	Ann ^c
LPFBT	376 (~440)	420, 540	384 (429)	389 (430)	530	534
HPF_B40	357	413	360	362	418 (441)	419 (441)
HPFBT_B5	372 (~440)	417, 539	378 (430)	384 (432)	529	533
HPFBT_B15	365 (~440)	415, 535	372	369	526	528
HPFBT_B40	325 (~440)	409, 513	332	333	508	508

^a Data in the parentheses are the wavelength of shoulders.

^b Obtained from the as-prepared films.

^c Films annealed at 200 °C in air for 1 h.

3.3. Optical properties

UV–vis absorption (UV) and photoluminescence (PL) data of the polymers are shown in Table 2 and Fig. 1. With the increase of branching degree of the polymers, UV and PL peaks were blue-shifted gradually from LPFBT to hyperbranched polymers with increasing BDs. This suggested that introduction of branching units (1,3,5-substituted benzene rings) interrupts the linear π -system to some extent. When the branching degree is not high, these UV and PL maxima of hyperbranched polymers (HPFBT_B5 and B15) were only slightly shifted with each other and close to the maximum of their model polymer (LPFBT). But when the BD was 40%, this change became much more obvious from 376 to 325 nm for UV and from 420 to 409 nm for PL in solution. Moreover, compared with the LPFBT and HPF_B40, the absorption and emission spectra of these copolymers with higher BDs, both as films and in solutions (see Figs. 1b and 2d) became broader and featureless. This may be attributed to the disorder of chain structure and conformation produced by highly branched structure and random distribution of BT units in the backbone. Thus this troubled state unfavorably affects the fine vibronic spectrum [29]. Moreover, the occurrence of self-absorption which is induced by polydispersity of chromophores with different effective conjugated lengths in this hyperbranched system [21,30], is also an important effect. All these mentioned above demonstrated that energy migration through hyperbranched structure had significant influences on the absorption and emission spectra. Meanwhile, the main absorption and emission peaks of HPFBT_B40 showed a large blue-shift (from 357 to 325 nm for UV and from 413 to 409 nm for PL in solution) compared with its counterpart HPF_B40, due to the decrease of conjugated length of the HPF_B40 segments interdicted by the BT unit. For the BT-based copolymers, a clear shoulder in Fig. 1a and 1b can be observed at ca. 440 nm both in solution and as solid-state films, which is responsible for the BT unit in the copolymers [31].

Fig. 1c shows that after annealing the solid-state films at 200 °C for 1 h in air, some weak long wavelength absorption tails appeared at about 450 nm in the absorption spectra of LPFBT and HPFBT_B5. Furthermore, the maximum peaks of their UV and PL spectra are shifted around 6 nm. On the contrary, there is no obvious change for the spectra of the

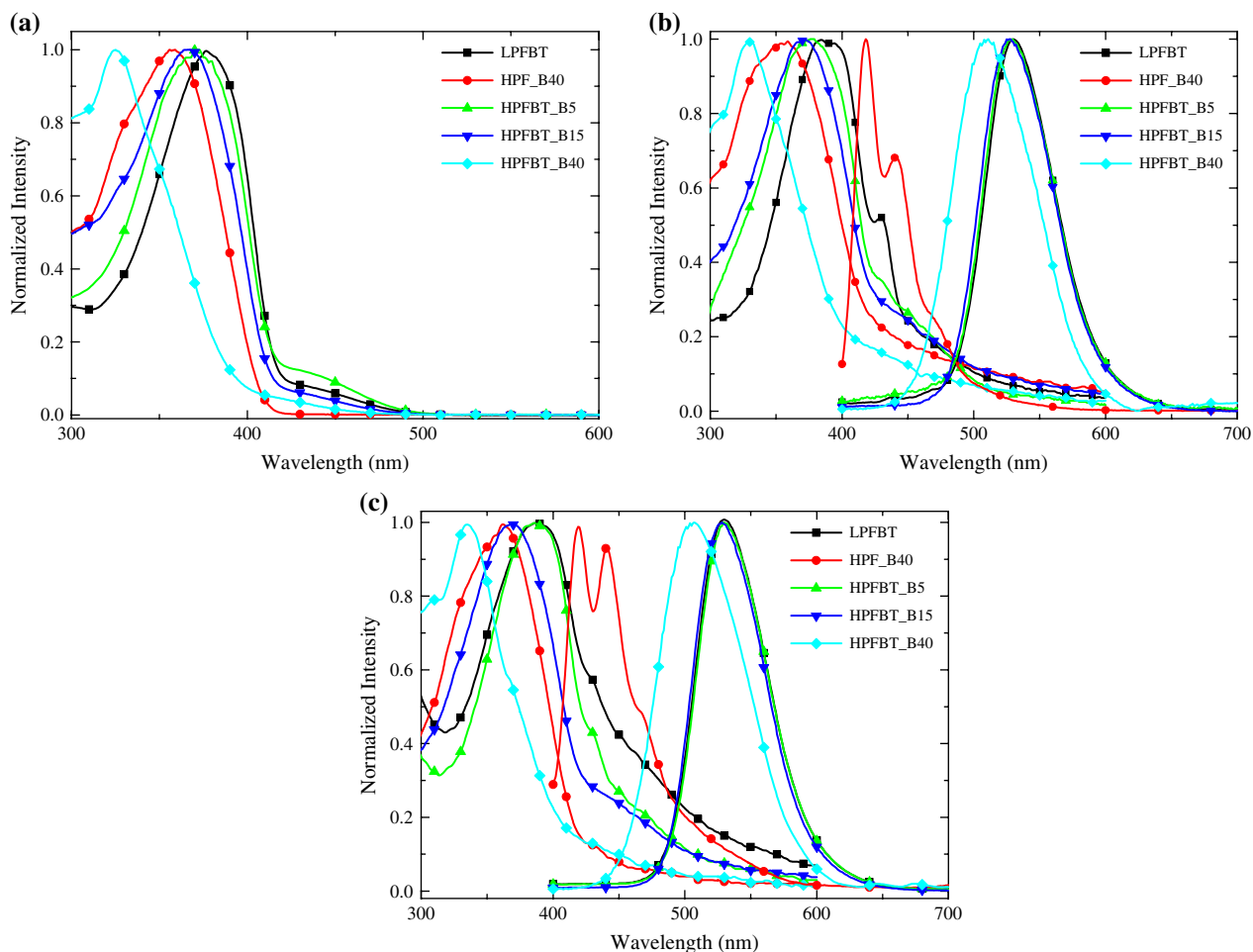


Fig. 1. (a) UV–vis absorption spectra of polymers in THF solution (around 6×10^{-6} mol/L); UV–vis absorption and PL emission of polymers: (b) as-prepared films and (c) as films annealed at 200°C in air for 1 h.

polymers with higher BDs. This result indicated that hyper-branched structure led to high thermal stability and it could prevent the aggregation and crystallization of the rigid polymer chain [32,33].

3.4. Energy transfer properties

In contrast to almost full energy quenching of wide band gap fluorene segments by BT unit in copolymer films, PL spectra in solution vary remarkably with the branching degrees and the solution concentration. Fig. 2 shows the normalized PL spectra of linear and hyperbranched BT-based copolymers in THF solutions. It is clear that the spectra have the concentration dependence in THF solutions. The emission of each copolymer at around 415 nm responsible for the polyfluorene (PF) segments decreases quickly with increasing copolymer concentration and the PF emission can be completely quenched in highly concentrated solutions. In Fig. 3, a plot of $I_{\text{BT}}/I_{\text{PF}}$ (ratio of the integrated intensities of 540 nm peak to that of 415 nm peak, which can be roughly considered as a measurement of energy transfer efficiency from fluorene segment to BT unit) [31] versus the concentration of the copolymers with different branching degrees is given. It can be found

that with the increase of branching degrees, the critical concentration C^* , at which the emissions from BT units begin to be quickly enhanced indicating the quickly increasing energy transfer among the polymers, rose gradually. The C^* obtained from Fig. 3 is 0.06, 0.069, 0.087, and 0.16 g/L for LPFBT, HPFBT_B5, B15, and B40, respectively. In contrast with photoluminescence spectra of these polymers as films (Fig. 1b), in which there are only peaks around 530 nm attributed to BT units emitting, the existence of critical concentration C^* and its value increasing with BDs (from 0 to 40%) seems to indicate that only intrachain interaction plays a major role in the energy transfer in dilute solution [31] and globular chain features led by highly branched structure suppress the intra- and interchain energy transfer effectively even in concentrated solution, reasons being described later.

Herein, for clear and convenient discussion of energy transfer in this hyperbranched system, two basic ideas are presented initially according to Schwartz's definition [34]. The first is that a conjugated polymer chain is that of a series of linked chromophores, each of which has a different extent of π -electron delocalization. The second is that the definition of interchain interactions implies only that π -electron density is delocalized between multiple conjugated segments, which

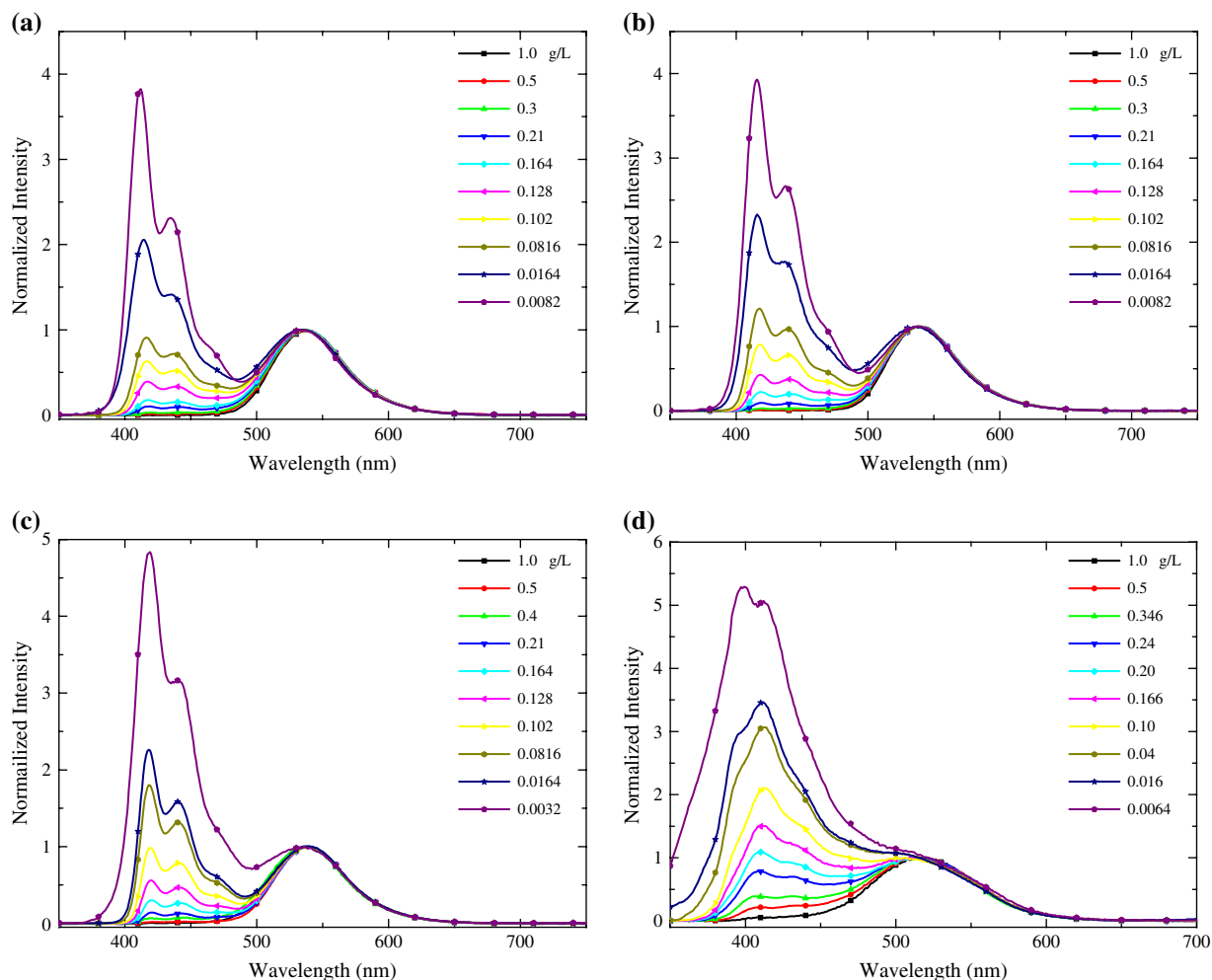


Fig. 2. PL spectra of polymers in THF solution with different concentrations. (a) LPFBT, (b) HPFBT_B5, (c) HPFBT_B15, and (d) HPFBT_B40.

does not depend on whether the interacting chromophores reside on physically distinct chains or are tethered together along the same polymer backbone. Therefore, because of the interruption of conjugated length by branching points (BPs), we approximately regard the segment between two BPs as

one chromophore and there are two probabilities of the composition of these chromophores. One just contains PF segment and the other contains both fluorene and BT units. Hence, three ways for energy transfer, i.e. no, intra- or interchain energy transfer, exist in this system as illustrated in Chart 1.

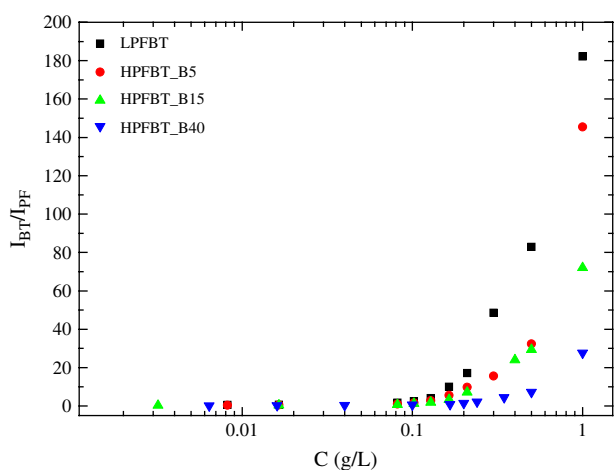


Fig. 3. I_{BT}/I_{PF} plotted against polymer concentration C for BT-containing polymers.

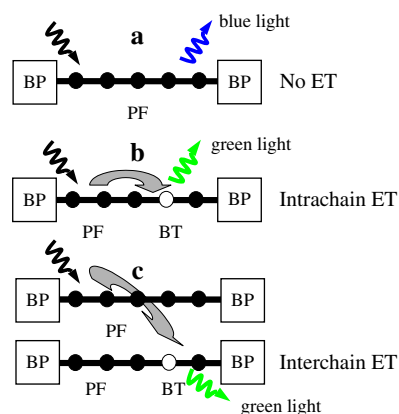


Chart 1. Illustration of intra- and interchain energy transfer (ET) among different chromophores – defined as the segment between two branching points (BPs), in this copolymer system.

Compared with linear form, hyperbranched structure breaks down the migration routes and hampers intrachain ET. Furthermore, the shape of these highly branched copolymers behaves in solution as hard sphere, therefore it is more difficult for the chains to be close to each other and the formation of entanglement even in concentrated solution [32]. Consequently, even when HPFBT and LPFBT solutions are in the same concentration, the neighboring distance of chromophores on HPFBT is much longer than that in LPFBT. It leads to quick decrease of interchain energy transfer. In addition, energy transfer between two chromophores on the same chain is the major process for interchain ET in solutions, and that highly branched structure also makes the chromophores on one polymer backbone further away from each other, which reduces the chance of interactions among them. That is the explanation why C^* rose with the increase of BDs.

However, for solid-state films, the intermolecular distance becomes very short and then interchain energy transfer, especially as two interactive chromophores are on two distinct chains, is a dominant way to quench the blue light emitting from PF completely. In Fig. 1b, either LPFBT or HPFBT with different BDs, shows one peak responsible for BT-containing chromophores.

Table 1 shows the PL efficiencies in the solid state, obtained from integrating sphere. The efficiency decreased quickly with the increase of BDs in these BT-based copolymers and HPFBT_B40 exhibited much lower efficiency than its counterpart HPF_B40. Moreover compared with the high photoluminescence efficiency (up to 46%) of linear poly(fluorene-*co*-benzothiadiazole), reported by Jen et al. [35], the efficiency of LPFBT in this paper (39%) is close to their result (much lower MW leads to relative disparity), but the efficiencies of those hyperbranched copolymers are much lower. This result is rather unique and interesting, since we initially presumed that the suppression of aggregation and excimer formation by hyperbranched structure would result in high PL efficiency. We suppose that the reasons mentioned above collectively to be responsible for this phenomenon. Firstly, hyperbranched structure leads to the complexity of chain configuration and the disorder of chain conformation. Such a large disorder parameter will give more defects and abrupt changes between chromophores which extremely damage the energy migration and bring some quenching sites in the polymers [36,37]. Secondly, the hyperbranched polymers have a much broader distribution of conjugation lengths which have been addressed by Xu and Pu [21]. In Fig. 1b, the relatively broader and featureless absorption and emission peaks of hyperbranched copolymers also demonstrate it. Thus, among chromophores with various efficient conjugation lengths, longer wavelength ones can present low energy states as trap sites leading to energy disorder and loss in the sample [38,39]. Therefore, in polymers with higher BDs, even those chromophores **a** as illustrated in Chart 1 will show more different conjugation lengths to enhance the occurrence of self-absorption and reduce efficiency. The feature of lower PL efficiency with higher BDs is consistent with the broad and featureless spectra of relevant polymers.

In one word, highly branched structure increases the complexity and possible ways of ET in the sample and affects the film morphology and polymer packing geometry [32,40] which also significantly influence the ET process and PL efficiency [41,42].

3.5. Electrochemical properties

Cyclic voltammetry (CV) was used to assess the electrochemical behavior of the polymers. The measurement was performed in a solution of *n*-Bu₄NPF₆ (0.1 M) in acetonitrile at a scan rate of 50 mV/s at room temperature under the protection of argon. A platinum electrode was coated with a thin polymer film and was used as the working electrode. A Pt wire was used as the counter electrode. A Ag/AgNO₃ electrode was used as quasi-reference electrode, which was calibrated using an internal standard, ferrocene/ferrocenium redox couple. The HOMO level was calculated according to an empirical formula, $E_{\text{HOMO}} = -e(E_{\text{ox}} + 4.84)$ (eV) [43]. And the band gaps (E_{gap}) were estimated from absorption onset of the polymers, thus, E_{LUMO} was calculated using the equation $E_{\text{LUMO}} = E_{\text{HOMO}} + E_{\text{gap}}$. All results are listed in Table 3.

As shown in Fig. 4, the polymers show a reversible oxidation wave with onset at around 0.92–1.02 V for BT-based copolymers and at 0.94 V for HPF_B40, which can be assigned to the oxidation potential of (co)polymer main chain. The band gap estimated from the onset wavelength of optical

Table 3
Electrochemical properties of linear and hyperbranched polymers films

Polymer	E_{ox} (V)	HOMO (eV)	LUMO ^b (eV)	E_{gap} ^a (eV)
LPFBT	0.92	−5.76	−3.14	2.62
HPF_B40	0.94	−5.78	−2.95	2.83
HPFBT_B5	0.95	−5.79	−3.11	2.68
HPFBT_B15	0.99	−5.83	−3.08	2.75
HPFBT_B40	1.02	−5.86	−2.88	2.98

^a Estimated from the onset wavelength of optical absorption in solid-state film.

^b Calculated using the equation $E_{\text{LUMO}} = E_{\text{HOMO}} + E_{\text{gap}}$.

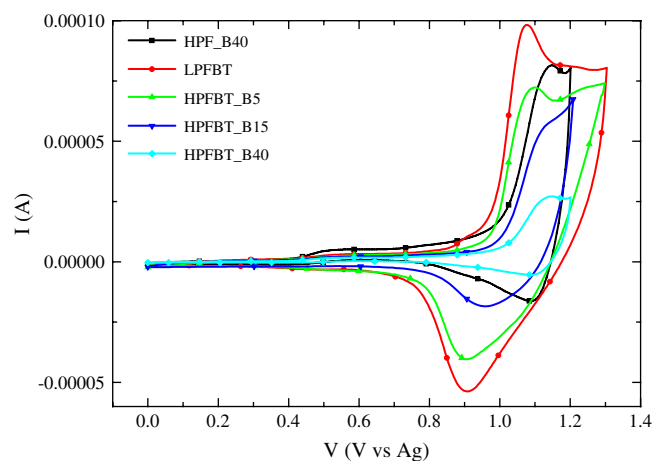


Fig. 4. Cyclic voltammograms of the polymers films coated on platinum electrodes in 0.1 mol/L Bu₄NPF₆/CH₃CN solution.

absorption as solid-state film increased with the branching degrees. From Table 3, the HOMO level decreased and LUMO level increased for higher branching degrees, which indicated more difficulty in hole or electron (charge) injection.

4. Conclusions

Linear and hyperbranched benzothiadiazole-based polyfluorene with branching degrees varied from 5 to 40% have been designed and synthesized using Suzuki coupling reactions. These polymers are thermally stable with T_d ranging from 280 to 376 °C, in accordance with the common advantages of hyperbranched structure. And less red-shift of UV or PL spectra of polymers with higher branching degrees also proved enough the thermal stability of hyperbranched structure. The absorption and emission peaks of these polymers are blue-shifted gradually with the increase of BDs. This suggested that introduction of branching units interrupted the linear π -system to some extent and reduced the effective conjugation length. Furthermore, the critical concentration C^* was used to scale the energy transfer properties in this system and its value increasing with BDs (from 0 to 40%) indicates that intrachain interaction plays a major role in the energy transfer in dilute solution and especially in these hyperbranched polymers with high BDs. However, as films, because of very close distance among all chromophores, only low band gap units (BT) emit luminescence around 520 nm. Cyclic voltammetry shows that hyperbranched structure in this system hinders the charge injection, which may result in low quantum efficiency for device application when highly branching degrees. More investigations on the time-resolved energy transfer process in these hyperbranched polymers and their applications are being conducted by our group.

Acknowledgements

This work was financially supported by the National Natural Science Foundation of China under Grants 60325412, 90406021, and 50428303 as well as the Shanghai Commission of Science and Technology under Grant 04XD14002 and the Shanghai Commission of Education under Grant 2003SG03.

References

- [1] Bernius MT, Inbasekaran M, O'Brien J, Wu P. *Adv Mater* 2000;12:1737–50.
- [2] Kim DY, Cho HN, Kim CY. *Prog Polym Sci* 2000;25:1089–139.
- [3] Kraft A, Grimsdale AC, Holmes AB. *Angew Chem Int Ed* 1998;37:402–28.
- [4] Scherf U, List EJW. *Adv Mater* 2002;14:477–87.
- [5] Redecker M, Bradley DDC, Inbasekaran M, Wu WW, Woo EP. *Adv Mater* 1999;11:241–6.
- [6] Jin YE, Kim JY, Park SH, Kim J, Lee S, Lee K, et al. *Polymer* 2005;46:12158–65.
- [7] Wu WC, Liu CL, Chen WC. *Polymer* 2006;47:527–38.
- [8] Cirpan A, Ding LM, Karasz FE. *Polymer* 2005;46:811–7.
- [9] Inbasekaran M, Wu W, Woo EP. U.S. Patent 5777070; 1997.
- [10] Hou Q, Xu YS, Yang W, Yuan M, Peng JB, Cao Y. *J Mater Chem* 2002;12:2887–92.
- [11] Peng Q, Lu ZY, Huang Y, Xie M, Han S, Peng J, et al. *Macromolecules* 2004;37:260–6.
- [12] Bredas J-L, Beljonne D, Coropceanu V, Cornil J. *Chem Rev* 2004;104:4971–5003.
- [13] Buckley AR, Rahn MD, Hill J, Gonzalez JC, Fox AM, Bradley DDC. *Chem Phys Lett* 2001;339:331–6.
- [14] Stevens MA, Silva C, Russell DM, Friend RH. *Phys Rev B* 2001;63:165213.
- [15] Westerling M, Vijila C, Osterbacka R, Stubb H. *Phys Rev B* 2003;67:19521.
- [16] Yu J, Lammi R, Gesquiere AJ, Barbara PF. *J Phys Chem B* 2005;109:10025–34.
- [17] Li J, Bo ZS. *Macromolecules* 2004;37:2013–5.
- [18] Tao XT, Zhang YD, Wada T, Sasabe H, Suzuki H, Watanabe T, et al. *Adv Mater* 1998;10:226–30.
- [19] Duan L, Qiu Y, He QG, Bai FL, Wang LD, Hong XY. *Synth Met* 2001;124:373–7.
- [20] Sun MH, Li J, Li BS, Fu YQ, Bo ZS. *Macromolecules* 2005;38:2651–8.
- [21] Xu MH, Pu L. *Tetrahedron Lett* 2002;43:6347–50.
- [22] He QG, Yan JL, Lin HZ, Zhang L, Song Y, Bai FL. *Polym Adv Technol* 2003;14:297–302.
- [23] Lightowler S, Hird M. *Chem Mater* 2004;16:3963–71.
- [24] Kim YH, Webster OW. *Macromolecules* 1992;25:5561–72.
- [25] Marsitzky D, Klapper M, Müllen K. *Macromolecules* 1999;32:8685–8.
- [26] Liu B, Bazan GC. *J Am Chem Soc* 2004;126:1942–3.
- [27] Katsis D, Geng YH, Ou JJ, Culligan SW, Trajkovska A, Chen SH, et al. *Chem Mater* 2002;14:1332–9.
- [28] Sarker AM, Kaneko Y, Lahti PM, Karasz FE. *J Phys Chem A* 2003;107:6533–7.
- [29] Chunwaschirasiri W, Tanto B, Huber DL, Winokur MJ. *Phys Rev Lett* 2005;94:107402.
- [30] Rauscher U, Bassler H, Bradley DDC, Hennecke M. *Phys Rev B* 1990;42:9830–9.
- [31] Huang F, Hou LT, Wu HB, Wang XH, Shen HL, Cao W, et al. *J Am Chem Soc* 2004;126:9845–53.
- [32] Voit B. *J Polym Sci Part A Polym Chem* 2005;43:2679–99.
- [33] Gao C, Yan D. *Prog Polym Sci* 2004;29:183–275.
- [34] Schwartz BJ. *Annu Rev Phys Chem* 2003;54:141–72.
- [35] Herguth P, Jiang XZ, Liu S, Jen AKY. *Macromolecules* 2002;35:6094–100.
- [36] Wang CF, White JD, Lim TL, Hsu JH, Yang SC, Fann WS, et al. *Phys Rev B* 2003;67:035202.
- [37] Grage MML, Wood PW, Ruseckas A, Pullerits T, Mitchell W, Burn PL, et al. *J Chem Phys* 2003;118:7644–50.
- [38] Vehse M, Liu B, Edman L, Bazan GC, Heeger AJ. *Adv Mater* 2004;16:1001–4.
- [39] Ding LM, Karasz FE. *J Appl Phys* 2004;96:2272–7.
- [40] Sheiko SS, Gauthier M, Moller M. *Macromolecules* 1997;30:2343–9.
- [41] Cadby AJ, Lane PA, Mellor H, Martin SJ, Grell M, Giebeler C, et al. *Phys Rev B* 2000;62:15604–9.
- [42] Khan ALT, Sreearunothai P, Herzx LM, Banach MJ, Koehler A. *Phys Rev B* 2004;69:085201.
- [43] Leeuw DM, Simenon MMJ, Brown AR, Einerhand REY. *Synth Met* 1997;87:53–9.